Cell Host & Microbe
Article

The Unfolded Protein Response Element IRE1α Senses Bacterial Proteins Invading the ER to Activate RIG-I and Innate Immune Signaling

Jin A. Cho,[1] Ann-Hwee Lee,[2,3] Barbara Platzer,[1] Benedict C.S. Cross,[5] Brooke M. Gardner,[6] Heidi De Luca,[1] Phi Luong,[1] Heather P. Harding,[5] Laurie H. Glimcher,[2,4] Peter Walter,[6,7] Edda Fiebiger,[1,2] David Ron,[5] Jonathan C. Kagan,[1,2] and Wayne I. Lencer[1,2,*]

[1]Department of Medicine, Division of GI Cell Biology, Boston Children's Hospital, Boston, MA 02115, USA
[2]Harvard Digestive Diseases Center, Harvard Medical School, Boston, MA 02115, USA
[3]Department of Pathology and Laboratory Medicine
[4]Department of Medicine
Weill Cornell Medical College, New York, NY 10065, USA
[5]University of Cambridge Metabolic Research Laboratories and NIHR Cambridge Biomedical Research Centre, Cambridge CB2 0QQ, UK
[6]Department of Biochemistry and Biophysics, University of California, San Francisco, CA 94158-2517, USA
[7]Howard Hughes Medical Institute
*Correspondence: wayne.lencer@childrens.harvard.edu
http://dx.doi.org/10.1016/j.chom.2013.03.011

SUMMARY

The plasma membrane and all membrane-bound organelles except for the Golgi and endoplasmic reticulum (ER) are equipped with pattern-recognition molecules to sense microbes or their products and induce innate immunity for host defense. Here, we report that *i*nositol-*re*quiring-1α (IRE1α), an ER protein that signals in the unfolded protein response (UPR), is activated to induce inflammation by binding a portion of cholera toxin as it co-opts the ER to cause disease. Other known UPR transducers, including the IRE1α-dependent transcription factor XBP1, are dispensable for this signaling. The inflammatory response depends instead on the RNase activity of IRE1α to degrade endogenous mRNA, a process termed regulated IRE1α-dependent decay (RIDD) of mRNA. The mRNA fragments produced engage retinoic-acid inducible gene 1 (RIG-I), a cytosolic sensor of RNA viruses, to activate NF-κB and interferon pathways. We propose IRE1α provides for a generalized mechanism of innate immune surveillance originating within the ER lumen.

INTRODUCTION

Mammalian cells have evolved diverse mechanisms of innate immunity to detect microbes in the extracellular space and upon invasion. Most involve pattern-recognition receptors (PRRs) that sense common pathogen-associated molecular patterns (PAMPs) defining broad classes of microbes. The PRRs include members of the Toll-like receptor (TLR), NOD-like receptor, and retinoic-acid inducible gene 1 (RIG-I)-like receptor families of proteins that survey various subcellular compartments for the presence of microbes and their associated products (Barton and Kagan, 2009). To date, PRRs have been found to survey the extracellular environment, the cytosol, various endosomes, mitochondria, and peroxisomes, and recently the nucleus (Li et al., 2012). With this diversity of potential sites for innate immune surveillance, it is surprising that two of the largest cellular organelles, the Golgi complex and endoplasmic reticulum (ER), have no known innate recognition system, even though some viruses and bacterial toxins traffic through these organelles en route to the cytosol.

Cholera toxin (CT) is the major virulence determinant of *Vibrio cholera*,and the prototypical member of a family of AB_5 subunit bacterial toxins that traverses the Golgi and ER to gain access to the cytosol (Sandvig et al., 1992). In the ER, a fragment of the CT A subunit, termed the A1 chain, unfolds and dissociates from the B subunit and retrotranslocates across the ER membrane, a process that exploits the machinery for ER-associated degradation (ERAD) of terminally misfolded proteins (Tsai et al., 2001). Once in the cytosol, the A1 chain refolds to become an ADP ribosyl transferase that causes disease.

Here, we used CT to reveal a potent role for the ER in innate host defense against extracellular microbes. The mechanism involves *i*nositol-*re*quiring-1α (IRE1α), one of three ER membrane proteins in metazoans that sense terminally misfolded proteins to induce the UPR (Ron and Walter, 2007). The canonical UPR, however, is dispensable for signaling in this pathway. Rather, the A1 chain selectively activates IRE1α to cleave endogenous messenger RNA (mRNA) into fragments that engage RIG-I, a key pattern recognition receptor for invading viruses. Activation of RIG-I leads to a NF-κB-dependent inflammatory response. We propose that IRE1α acts as the sensor for a generalized mechanism of innate immune surveillance that originates from within the ER lumen.

RESULTS

Rapid Innate Immune Signaling Response to CT In Vivo

To test whether host cells can innately sense CT upon entry into the ER, we prepared mutant toxins lacking catalytic activity

Table 1. Toxin-Induced Inflammatory Response in Mouse and Human Intestinal Epithelial Cells

	mRNA Expression (Fold Change over Untreated Controls)					
	Mouse Intestine: Whole Tissue (2 hr)		Mouse Intestine: IECs (2 hr)		Cultured Human Intestinal T84 Cells (4 hr)	
Gene Symbol	E/E	CTB	E/E	CTB	E/E	CTB
IL8/CXCL1	2.00	1.02	4.59	1.01	5.24	1.66
IL1B	1.41	1.13	2.70	0.88	5.09	1.81
TNFA	NC	NC	1.45	0.53	4.17	1.44
CCL20	2.40	0.61	NC	NC	2.50	1.69
IFNB1	1.42	1.33	NC	NC	1.71	1.09
NFKBIA	ND	ND	ND	ND	1.64	1.18

E/E, E110D/E112D enzymatically inert CT; CTB, B subunit only; IECs, intestinal epithelial cells; NC, no change detected; ND, not determined. Mean fold change is reported, n = 3 independent experiments; in all cases, a two-tailed t test between E/E and CTB is $p < 0.05$.

(termed E/E [Jobling and Holmes, 2001]) or unable to retrotranslocate (termed R192G [Tsai et al., 2001]) (Figures S1A–S1C available online). We also prepared a B subunit only toxin lacking the A subunit entirely (termed CTB). Each of these mutants was nontoxic when applied to human intestinal T84 cells in monolayer culture. None contained detectable amounts of bacterial lipopolysaccharide (LPS) as measured in mouse macrophages.

The enzymatically inactive E/E mutant and CTB toxins were administered by gastric gavage into BALB/c mice. Whole-tissue preparations of proximal intestine and isolated jejunal epithelial cells were analyzed for transcription of inflammatory genes by multiplexed direct quantification of individual mRNAs. Within 2 hr of toxin application, the enzymatically inactive E/E mutant, but not CTB, induced transcription of multiple inflammatory cytokines (Table 1). A similar inflammatory response was obtained when the toxins were applied to apical surfaces of human intestinal T84 cells in monolayer culture (Table 1). Thus, intestinal cells detect the enzymatically inert CT mutant E/E and respond by transcription of inflammatory genes, suggesting a form of innate immunity. CTB, lacking the A subunit entirely, was not active. Since only the A subunit co-opts ERAD to enter the cytosol, the result suggests that the inflammatory signal originates from inside the ER as it processes the A subunit for retrotranslocation or upon entry of the A1 chain into the cytosol.

The CT A Subunit Is Sensed upon ER Entry and Induces NF-κB-Dependent Responses

To determine how the A subunit induces the inflammatory response, we exposed the polarized human intestinal cell lines T84 and Caco-2 to the wild-type and mutant toxins, including the A subunit mutant that is strongly inhibited in retrotranslocation and essentially nontoxic (R192G [Saslowsky et al., 2010; Tsai et al., 2001; Wernick et al., 2010]). The inflammatory response was measured 4 hr later by real-time quantitative PCR (qPCR) for transcription of the cytokines interleukin-8 (IL-8) and IL-6 (Figures 1A and 1B) and by protein expression (Figure S1E). Only toxins containing the A subunit induced the inflammatory cytokines as observed in the mouse intestine. CTB was inactive. Higher concentrations of toxin induced 5- to 6-fold higher signals, implicating a dose effect (Figure S1F). Toxin entry into the ER was required, because blockade of retrograde vesicular transport from plasma membrane to ER by treatment with brefeldin A (BFA) (Fujinaga et al., 2003) completely inhibited signal transduction (Figure 1C). In this time frame, BFA had no detectable effect on signaling by basolaterally applied LPS (bLPS), showing that the BFA effect was specific for the cellular response to CT. The R192G mutant was active in both intestinal cell lines, indicating that the inflammatory signal originates from the ER lumen. Thus, intestinal epithelial cells sense the CT A subunit upon entry into the ER and induce inflammatory mediators.

Because the CT A subunit is unfolded by ER chaperones before retrotranslocation, we considered whether this might elicit the unfolded protein response (UPR) as suggested before (Dixit et al., 2008). This was evidenced by increased expression of the ER chaperone BiP 16 hr after intoxication (Figures S2A and S2B). The UPR has been linked to inflammatory signals via the Jun N-terminal kinase (JNK) and NF-κB pathways (Pahl et al., 1996; Urano et al., 2000). We found no evidence for activation of the JNK pathway (Figures S2C–S2F), but the NF-κB complex was activated. This was evidenced by immunoblot detection of the NF-κB p65 subunit in nuclear extracts of CT-treated (but not control) cells (Figure 2A). CTB did not cause nuclear translocation of p65, consistent with its lack of activity in the gene expression assays. Furthermore, immunoblot of total cell lysates for phospho-IKKα/β and phospho-IκBα showed that these upstream components of the NF-κB pathway were also activated by the holotoxins (A and B subunits assembled together), but not by CTB (Figure 2B). Finally, Bay11, a small-molecule inhibitor of IκBα activation, completely blocked the holotoxin-induced inflammatory cytokine response (Figure 2C). Thus, inflammatory signal transduction by the CT A subunit in the ER is NF-κB dependent.

The CT A Subunit Activates IRE1α, but Not the Canonical UPR

In metazoans, three transmembrane ER proteins are known to activate cytosolic responses to unfolded proteins in the ER lumen: IRE1α, PKR-like ER kinase (PERK), and activating transcription factor-6 (ATF6) (Ron and Walter, 2007). We found no evidence for activation of PERK or ATF6 (Figures S3A–S3E), but IRE1α was activated (Figures 3A–3C). This was assayed in total cell extracts by immunoblot for phosphorylated and non-phosphorylated forms of IRE1α using phos-tag SDS-PAGE. We found phospho-IRE1α in cells treated with all the holotoxins at 16 hr and at earlier times after intoxication with WT CT and the

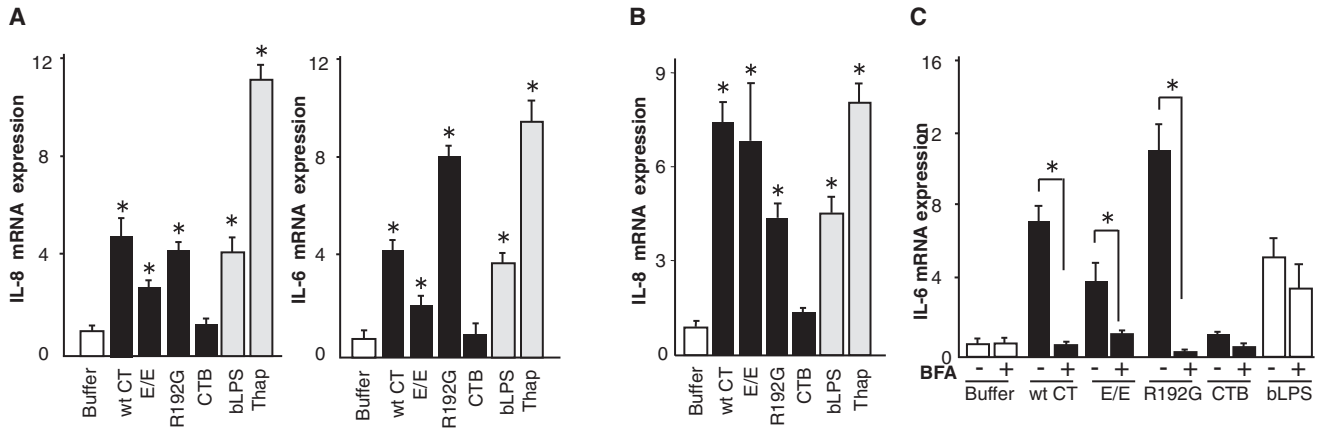

Figure 1. The CT A Subunit Induces IL-6 and IL-8 from within the ER

(A) Polarized T84 cells were intoxicated with 3 nM toxin for 4 hr, and IL-6 and IL-8 were assessed by real-time qPCR. The TLR4 agonist LPS (applied basolaterally, bLPS) and the ER stress-inducing agent thapsigargin (Thap) were used as positive controls.

(B) Polarized Caco-2 cells treated as in (A).

(C) Polarized T84 cells treated as in (A) with or without brefeldin A (BFA) pretreatment and assayed for IL-6 by real-time qPCR.

Open bars represent negative controls. Gray bars represent positive controls. wt CT, wild-type CT; E/E, E110D/E112D mutant; R192G, R192G mutant; CTB, B subunit alone. Data are shown as means ± SEM. *$p < 0.05$ by ANOVA. See also Figure S1.

R192G mutant (Figure 3A, slower migrating band). CTB did not induce phosphorylation of IRE1α at any time. Activation of IRE1α by the holotoxins was confirmed by real-time qPCR for the spliced RNA message of the transcription factor XBP1, which is cleaved to its active form by IRE1α upon activation (Ron and Walter, 2007). Spliced XBP1 was apparent starting 1 hr after intoxication and increased in abundance over time (Figure 3B). CTB was again completely inactive. XBP1 splicing induced by the R192G mutant, however, was not detected until 16 hr after intoxication, suggesting that XBP1 may not be required for the cytokine response. The delay in XBP1 splicing is perhaps explained by incomplete unfolding of the mutant R192G A1 chain within the ER lumen (Tsai et al., 2001). We also assayed for a downstream product of the IRE1α/XBP1 pathway, the ER chaperone ERdj4. All the holotoxins (but not CTB) induced transcription of ERdj4 by 16 hr after intoxication (Figure 3C). Thus, IRE1α was activated by the A subunit shortly after toxin entry into the ER, but PERK and ATF6 were not detectably activated.

To confirm the specificity for IRE1α in originating the inflammatory cytokine response, we first silenced expression of IRE1α and XBP1 in HeLa cells by stable transfection with short hairpin RNA (shRNA) against either IRE1α or XBP1. Strong depletion (>90%) of these proteins was shown by immunoblot (Figures 3D′ and 3E′). The cytokine response induced by the A subunit was assessed as described above (Figure 1). As expected, all the holotoxins caused expression of the inflammatory cytokines IL-6 and IL-8 in HeLa cells transfected with control shRNA against red fluorescent protein (shRFP), and there was no response to CTB (Figure 3D, left columns, and data not shown). However, in HeLa cells depleted of IRE1α, none of the toxins induced inflammatory cytokines (Figure 3D, right columns, shIRE1α) or nuclear translocation of p65 (Figure 3F, four lanes on left). IRE1α depletion did not interfere with intracellular trafficking of the toxins from the cell surface through the ER to the cytosol (Figure S3F), arguing against indirect effects on toxin signaling.

XBP1 is a major effector of IRE1α signaling and contributes to cytokine gene expression in LPS-stimulated macrophages (Martinon et al., 2010). In HeLa cells, however, although gene silencing of XBP1 enhanced the baseline expression of IL-6 and IL-8 (as observed before [Kaser et al., 2008]), this had no effect on toxin-mediated induction of the inflammatory cytokines (Figure 3E) or nuclear translocation of p65 (Figure 3F, four lanes to right).

The same results were obtained in independent studies using mouse embryonic fibroblasts (MEFs) prepared from animals completely lacking either IRE1α or XBP1 (IRE1α$^{-/-}$ or XBP1$^{-/-}$) (Figures 3G and 3H). As for XBP-1, MEFs lacking PERK also responded normally to intoxication by all the holotoxins (Figure 3I). The B subunit was inactive in all cases.

Thus, IRE1α is required for the inflammatory cytokine response induced by the CT A subunit. This is initiated by entry of the A subunit into the ER without requirement for enzymatic activity or for retrotranslocation of the A1 chain to the cytosol. XBP1, PERK, and ATF6, however, are dispensable, findings that define an unconventional activation of UPR modules for signal transduction initiated by the CT A subunit.

Regulated IRE1-Dependent Decay and RIG-I Transduce the Toxin-Recognition Signal from IRE-1α to NF-κB

How then does IRE1α signal to NF-κB after its activation by the A subunit in the ER lumen? IRE1α can also act as a promiscuous endonuclease degrading a subset of mRNA associated with the ER membrane (a process termed regulated IRE1-dependent decay, or RIDD (Hollien et al., 2009; Hollien and Weissman, 2006). To test RIDDs contribution to A subunit induction of inflammatory cytokines, we used a small-molecule selective inhibitor of IRE1α RNase activity, 4μ8C. 4μ8C does not block the kinase activity of IRE1α, nor does it affect the endonuclease activity of IRE1α-related RNase L or other elements of the UPR signaling cascades, but it efficiently interferes with RIDD and XBP1 splicing (Cross et al., 2012). Pretreatment with 4μ8C

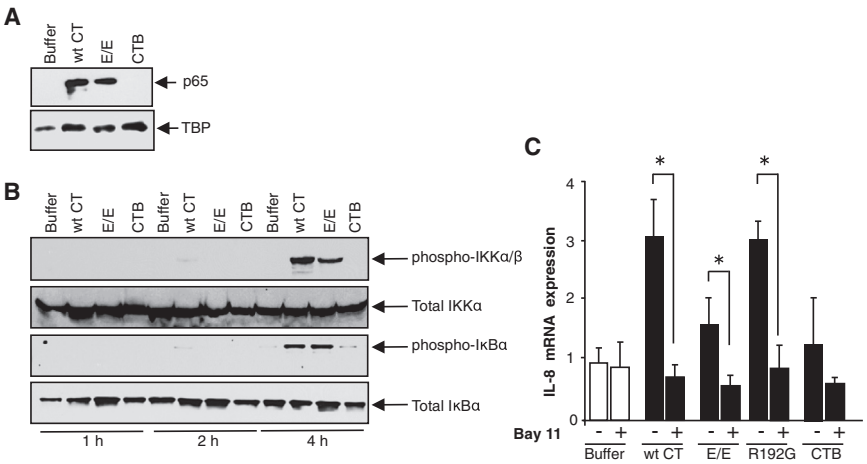

Figure 2. The Inflammatory Response Induced by CT A Subunit Is NF-κB Dependent

(A and B) Lysates of T84 cells were analyzed for nuclear translocation of p65 by immunoblot (A) and for phosphorylation of IKKα and IκBα (B). TATA-binding protein (TBP), total IKKα/β, and total IκBα are loading controls.

(C) T84 cells pretreated with NF-κB inhibitor Bay11 were intoxicated and analyzed for IL-8 by real-time PCR.

Data are shown as means ± SEM. Nomenclature is as described in Figure 1. See also Figure S2.

attenuated induction of the inflammatory cytokine response by the holotoxins, as measured by transcription of IL-8 and nuclear translocation of p65 (Figures 4A and 4B). There was no effect of 4μ8C on the IL-8 response by the TLR4 pathway (Figure 4A, last columns bLPS). We also found that transfection of IRE1α$^{-/-}$ MEFs with wild-type IRE1α rescued the cytokine response, but transfection with an IRE1α point mutant lacking endonuclease activity (IRE1 α-K907A) did not (Figure 4C); except for a small response to wild-type (WT) toxin that also induces cAMP. Thus, activation of NF-κB in cells exposed to CT requires the RNase activity of IRE1α but proceeds independently of XBP1 splicing.

This result implicates RIDD and degraded mRNA, or loss of gene expression, in signal transduction between IRE1α and NF-κB. IRE1 and the related endonuclease RNase L have similar catalytic mechanisms and generate mRNA fragments with 5′-OH and cyclic 2′,3′ phosphodiester 3′ ends (Dong et al., 2001; Gonzalez et al., 1999). RNase L mRNA degradation products have been observed to activate the RNA helicase RIG-I, which senses single- and double-stranded uncapped RNA and contributes to innate immunity against invading viruses (Malathi et al., 2007; Malathi et al., 2010), in part by activating NF-κB (Kawai and Akira, 2008). To test whether mRNA products of IRE1α might function in a similar signaling pathway, we first used a well-characterized RIG-I deficient human hepatocyte cell line, Huh 7.5, and its wild-type parent cell line (Huh 7.0). Huh 7.5 cells lacking a functional RIG-I were resistant to induction of the inflammatory cytokine IL-8 by intoxication with CT and its enzymatically inactive mutants, while Huh 7.0 cells were responsive (Figure 4D). Treatment with thapsigargin (which also acts as a potent intracellular [Ca^{2+}] agonist) induced equal expression of IL-8 in both WT and RIG-I-deficient Huh cell lines, showing that the NF-κB inflammatory pathways were intact. Thus, in Huh cells, signal transduction induced by CT between IRE1α and the cytokine genes appeared to be RIG-I dependent.

To determine whether the 5′-OH 3′,2′-cyclic phosphate mRNA fragments generated by IRE1α (Gonzalez et al., 1999) can act in this pathway to activate cytokine gene expression, we isolated mRNA from IRE1α knockout mouse cells and subjected it to cleavage in vitro with the truncated cytosolic kinase and RNase domain of human IRE1α expressed in and purified from insect cells. As a control, we performed the cleavage reaction in the presence of 4μ8C (Figure 4E). The low-molecular-weight RNA fragments thus produced, including cleavage products of ribosomal RNA (as reported for IRE1α cytosolic domains [Iwawaki et al., 2001]), were isolated by size fractionation, transfected into Huh 7.0 or 7.5 cells, and assessed for their ability to promote IL-8 mRNA expression. IL-8 levels increased in Huh 7.0 cells transfected with RNA fragments produced by digestion with IRE1α (Figure 4F). There was no IL-8 response in cells transfected with the low-molecular-weight RNA fraction of the digestion performed in the presence of 4μ8C or after mock digestion, indicating specificity for RNA fragments produced by IRE1α. Huh 7.5 cells that lack RIG-I did not respond to the transfected RNA but retained their ability to induce IL-8 mRNA in response to TNFα (Figure 4F). Thus, RNA fragments produced by IRE1α RIDD activity in vitro can mediate the induction of the cytokine genes by activation of RIG-I.

To confirm these results, we studied MEFs prepared from mice lacking RIG-I or the mitochondrial antiviral signaling protein (MAVS) that is required for signal transduction by RIG-I. We found that MEFs lacking RIG-I were resistant to induction of IL-6 mRNA by intoxication with CT and its enzymatically inactive mutants but retained their ability to induce IL-6 in response to TNFα (Figure 4G). The RIG-I$^{-/-}$ cells were also strongly resistant to the nonspecific RIG-I agonist poly(I:C) as expected, but we saw no evidence for activation of the RIG-I analog MDA5 using this preparation of poly(I:C) (Kato et al., 2008). Like the RIG-I$^{-/-}$ cells, MEFs lacking MAVS (MAVS$^{-/-}$) were resistant to induction of IL-6 by intoxication with the holotoxins. This was rescued (>10-fold) by stable transfection with wild-type MAVS (WT MAVS rescue) (Figure 4H). MEFs lacking the other RNA helicase MDA5 (MDA5$^{-/-}$), however, were responsive to intoxication with the holotoxins, indicating specificity for RIG-1 in sensing mRNA fragments produced by RIDD (Figure S4A). Thus, RIG-I and MAVS are required, but MDA5 is not.

We do note, however, that each of the holotoxins induced a small but detectable IL-6 response in MAVS$^{-/-}$ cells, above that of the CT B subunit alone, suggesting that RIG-I may not be the only sensor for RIDD or that the toxins may induce other inflammatory pathways in this cell line. We also note that RIDD activation of RIG-I induces nuclear translocation of the

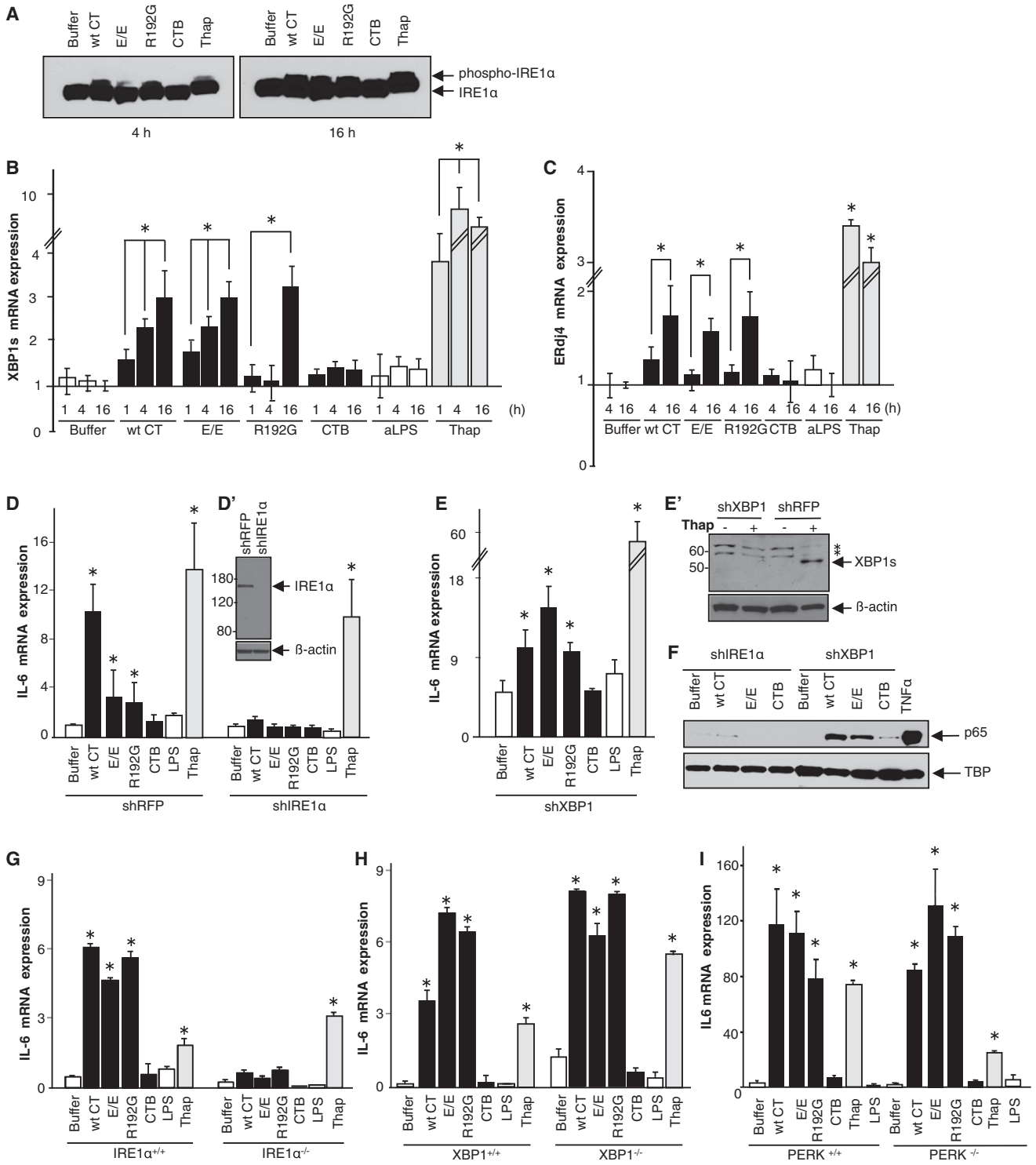

Figure 3. The CT A Subunit Activates the IRE1α Pathway, but XBP1 and PERK Are Dispensable

(A–C) T84 cells were intoxicated as indicated and analyzed for phospho-IRE1α (A), the spliced form of XBP1 mRNA (B), and ERdj4 mRNA (C). T84 cells treated with thapsigargin or apically applied LPS (aLPS) (or buffer alone) provided positive and negative controls, respectively.

(D–F) IRE1α or XBP1 was silenced in HeLa cells (D′ and E′). HeLa cells lacking IRE1α or XBP1 were intoxicated and analyzed for IL-6 mRNA expression by real-time PCR (D and E) and nuclear translocation of p65 by immunoblot (F). TBP and β-actin are loading controls.

(G–I) MEF cells lacking IRE1α (IRE1α$^{-/-}$; G), XBP1 (XBP1$^{-/-}$; H), or PERK (PERK$^{-/-}$; I) were intoxicated and analyzed for IL-6 mRNA expression by real-time PCR. Data are shown as means ± SEM. Nomenclature is as described in Figure 1. In (E′), * indicates nonspecific protein bands. See also Figure S3.

interferon transcription factor IRF3 (Figure 4I) and a small but IRE1α-dependent expression of interferon beta (IFNβ, Table 1 and Figures S4B–S4D) as would be expected for signal transduction by RIG-I.

To test whether our observations with CT may define a general rule for innate immune surveillance by the ER, we used the closely related AB_5 subunit Shiga toxin and SV40 virus. Like CT, both Shiga toxin and SV40 virus must enter the ER to induce disease. Here, we found that in MEFs expressing IRE1α, the enzymatically inactive mutant of Shiga toxin induced an IL-6 response, but the B subunit alone did not, and this was completely absent in MEF IRE1$\alpha^{-/-}$ knockout cells (Figure 5A). We also found that infection by SV40 virus in intestinal T84 and Caco-2 cells induced a strong IL-8 response that was inhibited by treatment with 4μ8C (Figure 5B). These results implicate signal transduction by RIDD and RIG-I. Thus, another bacterial toxin and a pathogenic virus entering the ER of host cells induce inflammation in the same way as CT. In contrast, enzymatically inactivated Diphtheria/Anthrax chimera toxins did not induce expression of the inflammatory cytokines after intoxicating intestinal T84 or Caco-2 cells (Figure 5C). Unlike CT, Shiga toxin, and SV40 virus, the chimera toxins enter the cytosol by translocating across endosome membranes. They do not traffic to the ER.

We also tested for the IRE1α-RIDD pathway in cells of hematopoietic lineages operating classically in innate immunity. Here, we found that macrophages isolated from WT mice responded to the CT A subunit by expression of inflammatory cytokines and this was dependent on RIDD as evidenced by inhibition with 4μ8C (Figure 5D). But macrophages isolated from mice lacking MAVs did not. These results in macrophages fully recapitulate our findings in epithelial cells and fibroblasts, further implicating a general rule for innate immune surveillance by IRE1α.

Activation of IRE1α by Toxin Binding

How does the CT A subunit activate IRE1α? Recent evidence suggests that in the UPR, the yeast homolog of IRE1α is activated by direct binding to unfolded proteins in the ER lumen (Gardner and Walter, 2011). Accordingly, the CT A subunit, which is unfolded in the ER prior to retrotranslocation, could specifically activate IRE1α by directly binding to the lumenal domain of IRE1α. To test this hypothesis, we probed an array of peptide sequences derived from tiling along the sequence of the CT A subunit for binding to the purified mouse Ire1α ER-lumenal domain (mIre1α-LD). The signal intensity attributed to each amino acid for binding Ire1α was averaged and normalized to a scale of 0–1 as described previously (Gardner and Walter, 2011). Two regions within the CT A subunit showed prominent binding to mIre1α-LD (Figures 6A and 6B). Both sites are located within the A1 chain (Figures 6A–6C), which is the fragment of the A subunit retrotranslocated to the cytosol (Tsai et al., 2001; Wernick et al., 2010). GST alone did not bind the array (data not shown), and the pattern of binding to the core lumenal domain of mouse PERK (mPERK-LD) was different. mPERK-LD bound prominently to one region in the A2 chain (uniquely to PERK) and one region in the A1 chain that partially overlapped with one of the IRE1α binding sites (K. Gotthardt and P.W., unpublished data).

We tested for direct protein-protein interaction by coimmunoprecipitation of the A1 chain with FLAG-tagged IRE1α stably transfected in HeLa cells. In cells treated with WT CT, the anti-FLAG antibodies immunoprecipitated IRE1α and the CT A1 chain (Figure 6D). This was blocked in cells treated with BFA that inhibits entry of the toxin into the ER. There was no detectable A1 chain signal in control HeLa cells lacking FLAG-tagged IRE1α or when the cells were not intoxicated. These results implicate a mechanism for IRE1α activation by direct binding to the unfolded CT A1 chain.

DISCUSSION

Our findings delineate a mechanism of innate immunity uniquely localized to the lumenal ER membrane. In response to the presence of a bacterial protein that is unfolded in the ER, IRE1α is activated to generate endogenous RNA ligands that engage an innate immune effector mechanism previously believed to be dedicated to antiviral defense (see the graphical abstract). RNase L, whose effector domain evolved from IRE1α by gene duplication (Bork and Sander, 1993), performs a similar task by generating RIG-I ligands to amplify signaling in virally infected cells. RIDD is absent from budding yeast and is first reported in animal cells (Hollien and Weissman, 2006). It seems likely, therefore, that IRE1's endonuclease activity is the ancestral function, duplicated and extended in RNase L, and utilized in animal cells for antibacterial and antiviral defense.

IRE1α, the most evolutionarily ancient regulator of the UPR, is selectively activated by the ER-localized CT A subunit; neither PERK nor ATF6 are detectably activated. Based on our results, we consider it likely that IRE1α binds specific sites in the unfolded A1 chain to cause activation of RIDD. The core lumenal domain of PERK also binds regions of the A subunit, but in a different pattern, binding a single predominant region in the A1 chain and a second site in the A2 chain, a region of the A subunit that does not engage ERAD and is not retrotranslocated to the cytosol. As we find no evidence that PERK is activated in vivo, this interaction may either not occur in living cells, perhaps due to steric accessibility of that portion of the A1 chain in the ER lumen, or, if it did occur, would not lead to productive PERK activation.

With two binding sites, it is possible that the A1 chain binds IRE1α with high avidity, perhaps even tethering adjacent IRE1 dimers to form higher oligomers. This might explain how CT rapidly activates only one arm of the ER stress modules. High-avidity binding might also account for how the small amounts of toxin entering the ER lumen of host cells can cause RIDD. It could also be that ER chaperones are required to facilitate binding of the A1 chain to IRE1α, imparting specificity to the binding reaction and activation of signal transduction by coincident detection.

Mechanisms of innate immunity emanating from the ER have not been previously recognized. Two recent reports show that signal transduction induced by TLRs can be affected by the ER stress response (Martinon et al., 2010), and conversely that the ER stress response accommodates cell survival in TLR-dependent innate immunity (Richardson et al., 2010). Neither paper, however, addresses the idea, or explains how the ER can act in sensing invasion of extracellular microbes and their products.

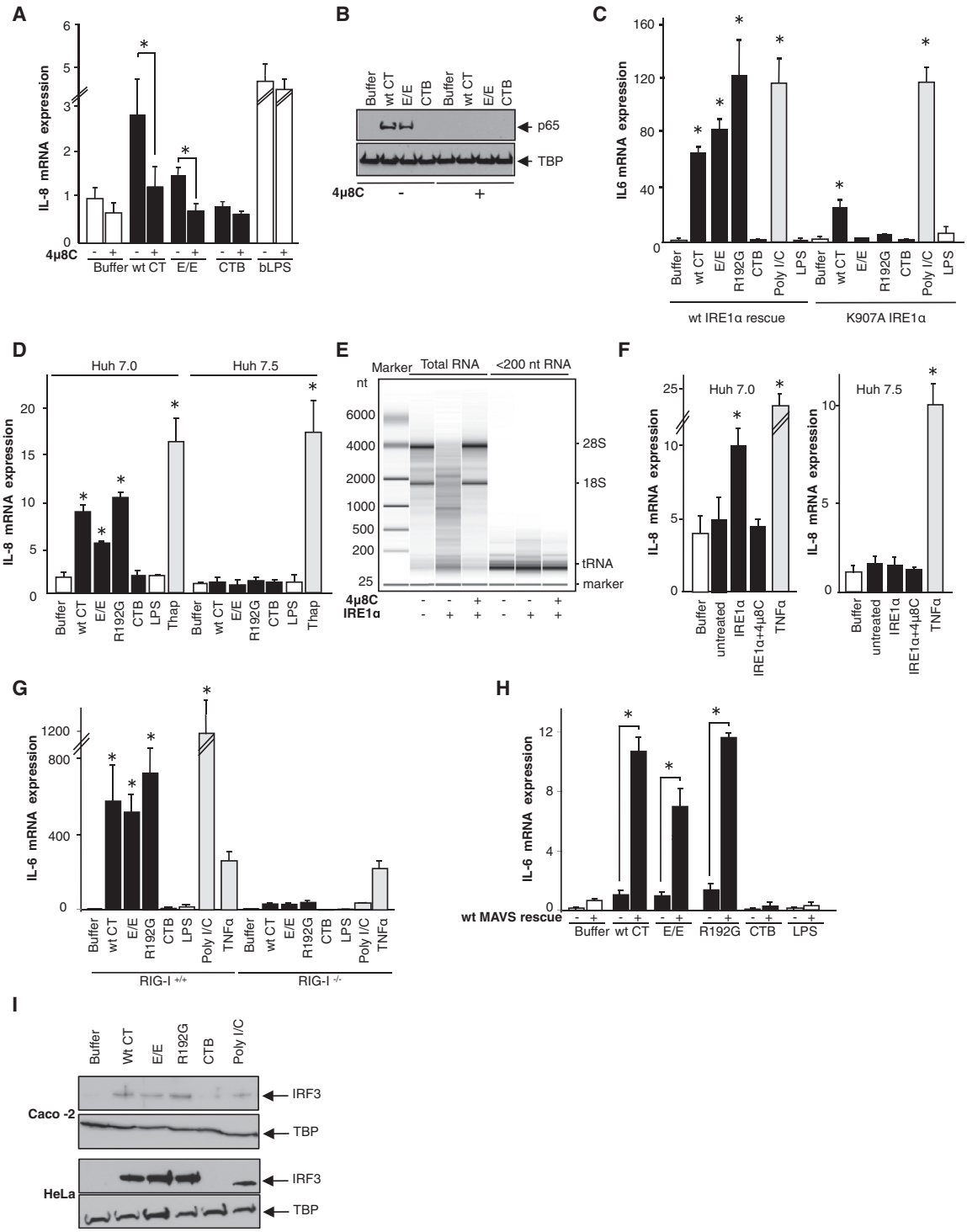

Figure 4. The Inflammatory Response Depends on the RNase Activity of IRE1α and on RIG-I, a Cytosolic Sensor of RNA Fragments

(A and B) T84 cells pretreated with 5 μM 4μ8C for 5 min were intoxicated and analyzed for transcription of IL-8 (A) and nuclear translocation of p65 (B). TBP is a loading control.

(C) Wild-type IRE1α rescued and K907A RNase domain-dead transfected IRE1α knockout MEFs were intoxicated and analyzed for transcription of IL-6.

(D) Huh 7.0 (WT) and Huh 7.5 (mutant RIG-I) cells were intoxicated and IL-8 mRNA was measured.

(E) Purified RNA from IRE1 knockout cells was digested with purified cytosolic domain of human IRE1α in the presence or absence of 4μ8C.

(F) Low-molecular-weight fragments of mRNA produced in vitro were transfected in Huh 7.0 (WT) and Huh 7.5 (mutant RIG-I) cells for 16 hr and IL-8 mRNA was assessed.

(G) Wild-type primary MEFs (RIG-I$^{+/+}$) or immortalized MEFs lacking RIG-I (RIG-I$^{-/-}$) were intoxicated, and IL-6 mRNA was measured.

(legend continued on next page)

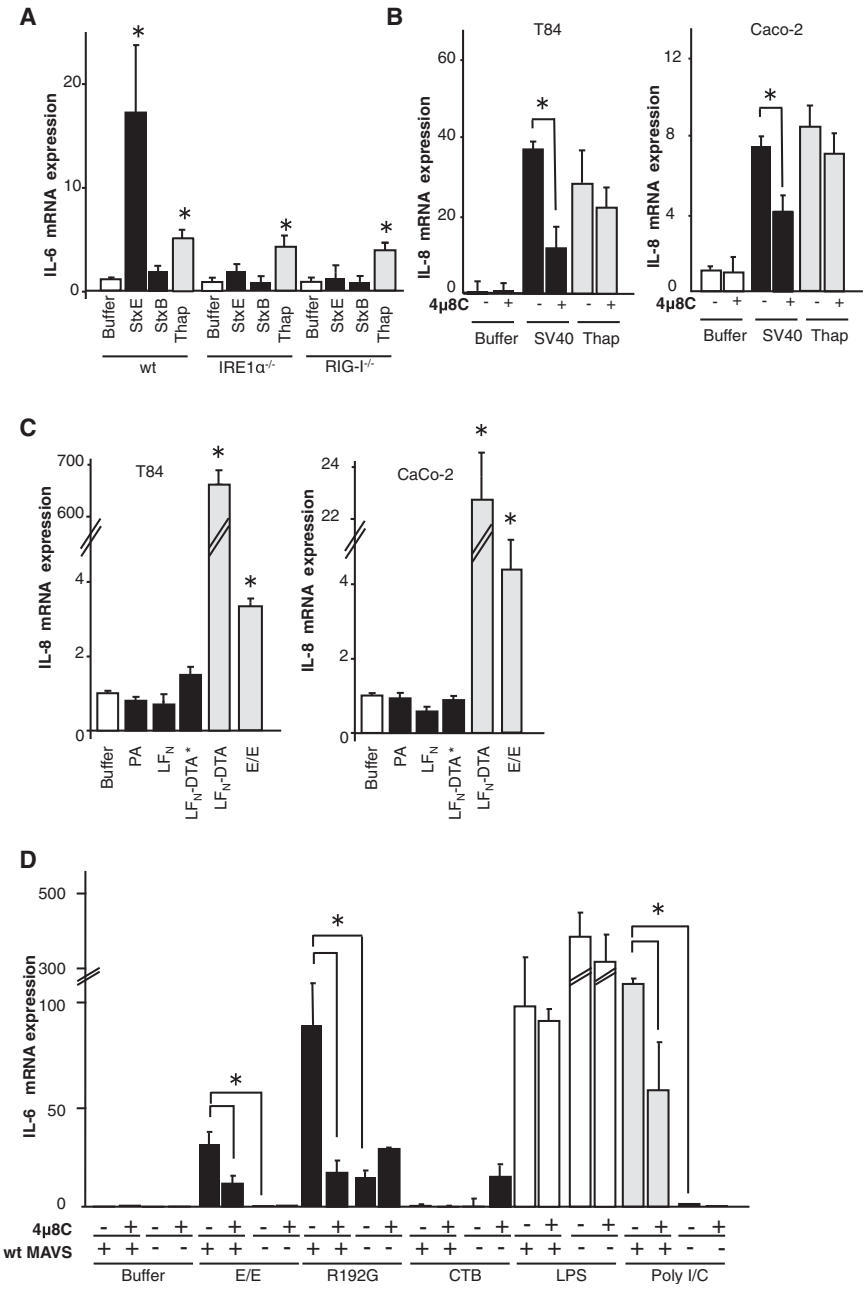

Figure 5. The IRE1-RIDD Pathway Defines a General Rule for Innate Immune Surveillance by the ER

(A) Wild-type MEFs or MEFs lacking IRE1α (IRE1α$^{-/-}$) or RIG-I (RIG-I$^{-/-}$) were intoxicated with an enzymatically inactive Shiga toxin mutant (StxE) or its B subunit alone (STxB), and IL-6 mRNA was quantified.

(B and C) T84 or Caco-2 cells pretreated or not with 4μ8C were infected with SV40 virus (B) or Anthrax-fused Diphtheria (C) for 4h and immune responses were assessed by qPCR.

(D) Wild-type macrophages or MAVS knockout macrophages pretreated or not with 4μ8C were intoxicated with toxins for 4 hr and analyzed for IL-6 by qPCR.

Data are shown as means ± SEM. PA, protective antigen; LF_N, amino-terminal 255 residues of lethal factor; LF_NDTA*, fusion protein composed of LF_N and the inactive catalytic domain of diphtheria toxin; LF_NDTA, fusion protein composed of LF_N and the catalytic domain of diphtheria toxin. Other nomenclature is as in Figures 1 and 4.

the canonical UPR appear to be involved, suggesting a form of pattern recognition.

It is not readily apparent, however, how the unfolded A1 chain fits the classic definition of a PAMP. The motifs on the A1 chain implicated in binding IRE1α are located on the surface of the molecule when in its folded conformation (Figure 6C), and like other well-established PAMPs (DNA or RNA), the peptide sequences when taken out of context are not uniquely microbial. We presume that specific binding to the MHC-class-I-like groove of IRE1α (Credle et al., 2005) can only occur when the A1 chain is unfolded. The CT B subunit enters the ER along with the A1 chain, but the B subunit is not unfolded and does not bind or activate IRE1α to activate RIDD. Small amounts of unfolded proteins, however, are present in the ER at all times. Perhaps the signature feature of the CT A1 chain is regions of the protein that allow unfolding upon entry into the ER and then refolding upon retrotranslocation to the cytosol, the opposite pattern for protein folding in the biogenesis and quality control of endogenous proteins. This is a feature fundamentally required of the bacterial and viral proteins that co-opt the ER for causation of disease. Other factors may be that the A1 chain acts only on the IRE1α branch of the ER stress sensors.

The reaction we describe is also distinct from the recently described pathway for induction of inflammation by the related *E. coli* AB_5 subunit subtilase toxin. Subtilase toxin enters the ER of host cells like CT, but then causes severe damage by enzymatic degradation of BiP to induce massive ER stress. In contrast, IRE1α senses entry of CT into the ER in the absence of cell damage. Neither the process of retrotranslocation nor

(H) MEF cells lacking the scaffolding protein MAVS (MAVS$^{-/-}$) and the same cells rescued by transfection with wild-type MAVS (wt MAVS rescue) were intoxicated, and IL-6 mRNA was measured.

(I) Caco-2 and HeLa cells were intoxicated and analyzed for nuclear translocation of IRF3 by immunoblot. TBP is a loading control.

Poly(I:C) and TNFα were used as positive controls. Data are shown as means ± SEM. Nomenclature is as in Figure 1. See also Figure S4.

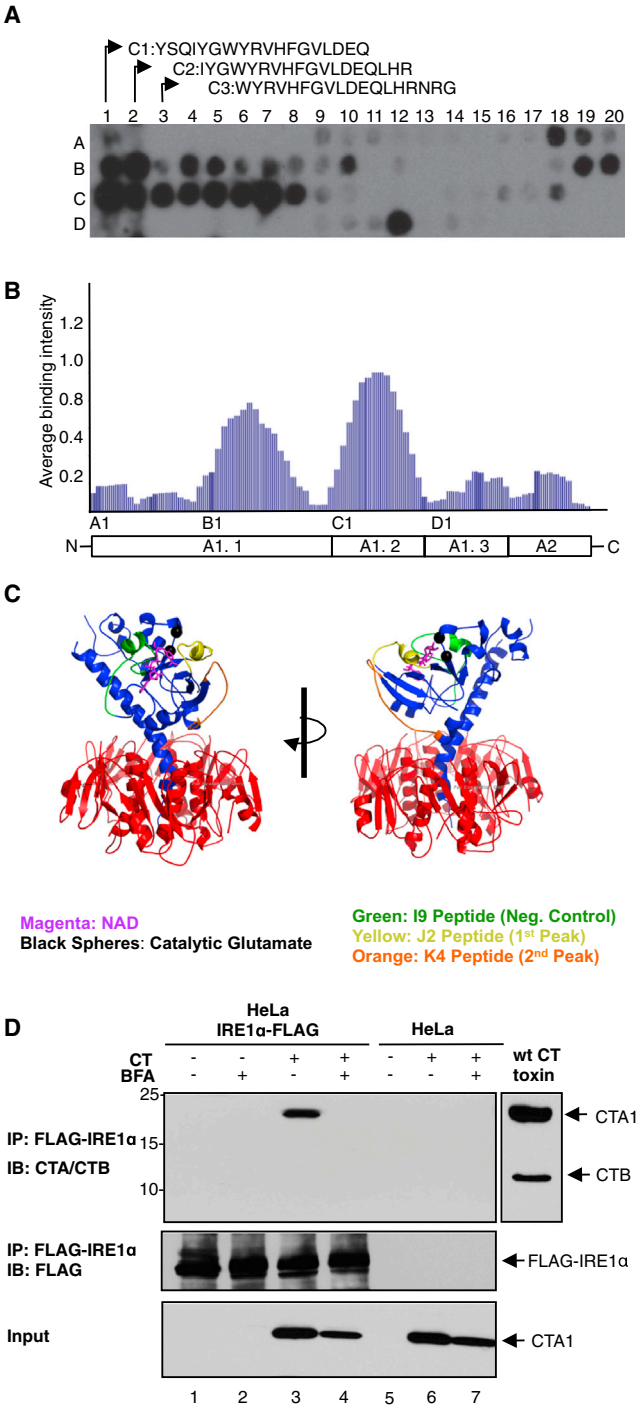

Figure 6. The Luminal Domain of Mouse IRE1α Binds Two Motifs in the CT A1 Chain

(A) An array of 18-mer peptides derived from the CT A subunit was incubated with purified mIre1α tagged with GST, and binding was detected with anti-GST antibodies.

(B) The contribution of each amino acid to binding mIre1α was plotted along the sequence of the CT A subunit from the N to C terminus, revealing two distinct GST-mIre1α binding sites.

(C) The cholera toxin crystal structure. The motifs that appear to bind IRE1α are on the external surface of the A1 chain (residues highlighted in yellow and orange).

(D) HeLa cells expressing FLAG-tagged IRE1α were intoxicated with WT CT in the presence or absence of BFA. IRE1α was immunoprecipitated and analyzed by immunoblot with antibodies against the CT A and B subunits (upper panel) and FLAG (middle panel). Total cell lysates were also immunoblotted for the A1 chain to provide additional controls (lower panel).

The features of toxin-induced IRE1α-mediated activation of RIG-I are also interesting in light of the known properties of RIG-I in initiating interferon (IFN) responses against invading viruses. We observe a small IRE1α-dependent IFN response in the studies described here, and stronger cytokine response initiated by NF-κB. Thus, the RIG-I/MAVS complex may differentially effect each signaling cascade as suggested before (Poeck et al., 2010), perhaps by discerning the activating ligand structures or the ligand concentrations. The activating ligands for natural RLR signal transduction are not yet fully defined with clarity (Loo and Gale, 2011; Rehwinkel and Reis e Sousa, 2010). In contrast, the cleavage products of IRE1 endonuclease activity (RIDD) are well delineated—they are single-stranded mRNA fragments with 5′-OH and a 2′,3′-cyclic phosphate terminus (Gonzalez et al., 1999). Our results implicate these fragments as activating ligands for RIG-I. The same 5′-OH and 2′,3′-cyclic phosphate mRNA fragments produced by RNase-L after viral infection also activate RIG-I (Malathi et al., 2007).

Mammals have a second isoform of IRE1 (IRE1β) whose expression is restricted to the heavily microbial colonized epithelium of the gut and whose absence predisposes to colitis (Bertolotti et al., 2001). We hypothesize the CT A1 chain also interacts with the lumenal domain of IRE1β, possibly with greater affinity, allowing for an augmented response. IRE1β's restricted expression and the finding that its RIDD activity is enhanced compared to its sequence-specific XBP1 splicing activity (Imagawa et al., 2008) suggest that mammals may broadly utilize RIDD-dependent immune surveillance, with strong amplification in the intestine that constitutes the essential interface between the host and hundreds of trillions of gut microbes.

EXPERIMENTAL PROCEDURES

Plasmids, purification, and other reagents used, as well as detailed experimental procedures can be found in the Supplemental Experimental Procedures.

Cell Culture

Human intestinal epithelial T84 cells (ATCC) were cultured as previously described (Lencer et al., 1992). Cells were incubated with 3 nM WT or mutant CT apically and 300 ng/ml LPS apically as negative or basolaterally as positive control, or 3 μM thapsigargin and 10 ng/ml recombinant human TNFα apically and basolaterally at various time points. Where indicated, intestinal T84 cells were pretreated with 5 μM brefeldin A or with 25 μM Bay 11 for 30 min. Human cervical epithelial HeLa cells transfected with shRNA against IRE1α or XBP1 were cultured in Dulbecco's modified Eagle's medium (DMEM) supplemented with 10% fetal bovine serum (FBS) and 2 μg/ml puromycin. HeLa cells were preloaded with 4 μM GM1 purified from bovine brain (a generous gift from David Ullman, VA Hospital, Bedford, MA) for 45–90 min at 37°C before addition of toxins. Human hepatocyte Huh 7.0 and 7.5 and MEFs from wild-type and mutant mice (IRE1α knockout, XBP1 knockout, PERK knockout, RIG-I knockout, and MAVS knockout) were previously described (Lindenbach et al., 2005; Lee et al., 2003; Sun et al., 2006; Urano et al., 2000). HEK293T and Huh cells and MEFs were maintained in DMEM supplemented with 10% FBS.

Preparation of Low-Molecular-Weight RNA Species

Total cellular RNA from IRE1α/β-deleted cells was collected and harvested by solvent extraction with RNAstat60, according to the manufacturer's instructions (AMSbio). RNA (250 μg) was incubated with or without 2 μM human IRE1α [464–977] purified from insect cells, as described previously (Cross et al., 2012), in the presence or absence of 64 μM 4μ8C for 1 hr at 30°C. Low-molecular-weight RNA fragments (<200 nt) were isolated by mirVana glass fiber filtration, according to the manufacturer's instructions (Invitrogen). IRE1α-mediated RNA digestion was confirmed by microfluidic capillary electrophoresis with a Bioanalyzer (Agilent).

Peptide Arrays

A peptide array of 18-mers tiling through the cholera toxin A subunit by 3 aa at a time was purchased from the MIT Biopolymers Laboratory (Cambridge, MA). The array was incubated in methanol for 10 min and then in binding buffer (50 mM Tris [pH 7], 150 mM NaCl, 10% glycerol, 2 mM DTT, and 0.02% Tween-20) for three 10 min washes. After 1 hr incubation at room temperature with 1 μM GST-mIre1α, the array was washed three times for 10 min in binding buffer to remove unbound protein. Using a semidry transfer apparatus, bound GST-mIre1α was transferred to a nitrocellulose membrane and detected with α-GST tag antibody (Abcam). Intensities were quantified with ImageQuant Array analysis software with background subtraction for a spot containing no peptide. For calculation of the contribution of each amino acid to GST-mIre1α binding, the intensity of each spot containing a particular 3 aa tile was averaged. Average spot intensities were normalized to the maximum spot intensity for each array.

Quantitative Real-Time qPCR

Total RNA of cells was extracted with the RNeasy mini kit (QIAGEN). Complementary DNA was prepared from total RNA with the Superscript first-strand synthesis system (Invitrogen) with the oligo $(dT)^{12-18}$ primers, according to the manufacturer's instructions. RNA samples were treated with DNase I (Invitrogen) for the elimination of genomic DNA. Cytokine mRNA expression was determined by real-time qPCR with relative quantitation by the comparative threshold cycle number (Ct) method, iCycler, and SYBR Green Ready-mix (Bio-Rad) and normalized by housekeeping gene (β-actin or GAPDH).

Preliminary experiments were performed with each primer pair to determine the amplification temperature that provided an optimal correlation between template concentration and signal intensity. At least three independent experiments were performed for each assay.

Intestinal Epithelial Cell Isolation from Mice

BALB/c mice (littermates, 6–8 weeks old) were obtained from The Jackson Laboratory. All procedures were approved by the Boston Children's Hospital Institutional Animal Care and Use Committee. Mice were treated with 50 μg toxin in PBS by intragastric feeding following a 3 hr starvation. The mice were sacrificed, and the small intestine was immediately taken out and flushed with ice-cold PBS. The proximal small intestine was cut into 3 cm pieces, and Peyer's Patches were removed. For multiplexed mRNA detection, 0.5 μg whole tissue (stored in RNAlater solution from Ambion) was homogenized in RLT buffer (QIAGEN) supplemented with β-mercaptoethanol using the gentleMACS Dissociator (Miltenyi Biotech). Nanostring nCounter analysis was performed by the Harvard Digestive Diseases Center Epithelial Cell Biology Core. For isolation of intestinal epithelial cells (IECs), pieces of the intestine were washed three times in ice-cold PBS and were incubated with 1 mM DTT in HBSS for 10 min in order to remove mucus in the lumen. After three washes with ice-cold PBS, pieces were incubated in 1 U/ml Dispase (Roche) in RPMI media for 30 min at 37°C. The isolated epithelial cells were collected by filtration through a 100 μm cell strainer (BD Bioscience) and centrifugation for 5 min at 1,500 rpm at 4°C. The cells were resuspended in 5 ml 100% Percoll (GE Healthcare), followed by layering with 8 ml 40% Percoll in RPMI. Cells were centrifuged for 20 min at 1,500 rpm without braking, and IECs were collected from the top 30% and washed with RPMI for the RNA extraction as described above.

Nanostring Analysis with nCounter

The NanoString nCounter gene expression system (NanoString Technologies) was used to quantify individual mRNA transcripts. In brief, RNA was extracted from polarized T84 cells, mouse IECs, or mouse whole-tissue preparation previously homogenized in RLT buffer. For hybridization, RNA or homogenate was incubated for 16 hr with the Codeset and loaded into the nCounter prep station, followed by quantification with the nCounter Digital Analyzer. So that side-by-side comparisons of nCounter experiments could be made, the nCounter data were normalized in two steps. The positive spiked-in controls provided by the nCounter instrument were used as per the manufacturer's instructions, and the copy numbers were normalized by five housekeeping genes (β-actin, B2M, GAPDH, HPRT1, and RP13A).

Immunoblot Analyses

Cells were lysed with RIPA lysis buffer (20 mM Tris [pH 7.5], 150 mM NaCl, 1% NP-40, 0.1% SDS, and 0.5% sodium deoxycholate) supplemented with EDTA-free protease inhibitor cocktail tablet or phosphatase inhibitor cocktail tablet (Roche) by incubation on ice for 1 hr. The total lysate was then clarified by centrifugation at 14,000 rpm for 20 min at 4°C. The supernatants were collected, and protein concentration was determined via the BCA procedure as described by the manufacturer (Pierce). Equal amounts of protein (15–30 μg total cell lysate) were mixed with reducing Laemmli SDS sample buffer, boiled, and resolved by SDS-PAGE, followed by transfer to a nitrocellulose membrane. Antigens were detected with the appropriate antibody followed by enhanced chemiluminescence (ECL) according to the manufacturer's instructions (Pierce).

Phos-Tag Gels

Phos-tag gels were made in the same way as the immunoblot described above except (1) 6.5% SDS-PAGE containing 10 μM Phos-tag (NARD Institute) and 10 μM $MnCl_2$ were used and (2) gels were soaked in 1 mM EDTA for 10 min before transfer onto a polyvinylidene difluoride membrane.

Nuclear Extraction

T84 cells were harvested from 6-well plate inserts and washed twice with PBS. Cells were resuspended in 80 μl cold hypotonic buffer (10 mM HEPES [pH 7.9], 10 mM $MgCl_2$, 10 mM KCl, and 0.5 mM DTT) supplemented with EDTA-free protease inhibitor and incubated on ice for 15 min, followed by addition of 25 μl 10% NP-40. The pellet was spun at 12,000 rpm for 30 s at 4°C and resuspended in 50 μl extraction buffer (20 mM HEPES [pH 7.9], 1.5 mM $MgCl_2$, 400 mM NaCl, 25% glycerol, 0.2 mM EDTA, and 0.5 mM DTT) supplemented with EDTA-free protease inhibitor. The supernatant was collected by centrifugation for 5 min at 4°C and loaded onto the SDS-PAGE gel.

Coimmunoprecipitation

HeLa cells stably overexpressing FLAG-IRE1α were loaded with 4 μM GM1 and intoxicated with 40 nM WT CT for 90 min in the presence or absence of a 10 μM BFA 30 min pretreatment. Cells were lysed with M-PER lysis buffer (Pierce) supplemented with EDTA-free protease inhibitor cocktail tablet and phosphatase inhibitor cocktail tablet by incubation on ice for 10 min. The total lysate was then clarified by centrifugation at 14,000 rpm for 20 min at 4°C. The supernatants were collected and precleared with mouse IgG-agarose (Sigma). The protein concentration was determined via the BCA procedure as described by the manufacturer. Equal amounts of the protein lysate were incubated with anti-FLAG-agarose beads (Sigma) overnight at 4°C and washed with washing buffer (25 mM Tris [pH. 7.2] and 0.15 M NaCl). The beads were boiled in the absence of reducing reagent first to release the protein complex, then 100 mM DTT was added and heated at 70°C for 5 min. The supernatant was resolved by SDS-PAGE followed by transfer to a nitrocellulose membrane. Antigens were detected with the CTA antibody followed by enhanced chemiluminescence (ECL).

Statistical Analysis

All data are representative of at least three independent experiments. Data are shown as mean ± SEM unless otherwise indicated. Statistical significance of comparison between two groups was determined by two-tailed Student's t test where indicated. For comparison of more than one group, one-way ANOVA was used. Significant differences were considered at p values of less than 0.05.

SUPPLEMENTAL INFORMATION

Supplemental Information includes four figures and Supplemental Experimental Procedures and can be found with this article online at http://dx.doi.org/10.1016/j.chom.2013.03.011.

ACKNOWLEDGMENTS

This study was supported by NIH grants DK48106, DK084424, and DK090603 and Harvard Digestive Diseases Center grant P30 DK34854 (W.I.L.); DK083894 and a CCFA Fellowship (J.A.C.); a Pathogenesis of Infectious Disease Award from the Burroughs Wellcome Fund and AI093589 (J.C.K.); R01AI075037 (E.F.); 1K01DK093597-01A1(B.P.); R01DK082448 (L.H.G.); R01DK089211 (A-H.L); and a Wellcome Trust Principal Research Fellowship (084812/Z/08/Z; D.R.). P.W. is an investigator of the Howard Hughes Medical Institute. We thank James DeCaprio for the gift of SV40 virus and Andrew McCluskey and John Collier for the gift of recombinant Diphtheria toxins.

Received: October 10, 2012
Revised: February 20, 2013
Accepted: March 25, 2013
Published: May 15, 2013

REFERENCES

Barton, G.M., and Kagan, J.C. (2009). A cell biological view of Toll-like receptor function: regulation through compartmentalization. Nat. Rev. Immunol. *9*, 535–542.

Bertolotti, A., Wang, X., Novoa, I., Jungreis, R., Schlessinger, K., Cho, J.H., West, A.B., and Ron, D. (2001). Increased sensitivity to dextran sodium sulfate colitis in IRE1beta-deficient mice. J. Clin. Invest. *107*, 585–593.

Bork, P., and Sander, C. (1993). A hybrid protein kinase-RNase in an interferon-induced pathway? FEBS Lett. *334*, 149–152.

Credle, J.J., Finer-Moore, J.S., Papa, F.R., Stroud, R.M., and Walter, P. (2005). On the mechanism of sensing unfolded protein in the endoplasmic reticulum. Proc. Natl. Acad. Sci. USA *102*, 18773–18784.

Cross, B.C., Bond, P.J., Sadowski, P.G., Jha, B.K., Zak, J., Goodman, J.M., Silverman, R.H., Neubert, T.A., Baxendale, I.R., Ron, D., and Harding, H.P. (2012). The molecular basis for selective inhibition of unconventional mRNA splicing by an IRE1-binding small molecule. Proc. Natl. Acad. Sci. USA *109*, E869–E878.

Dixit, G., Mikoryak, C., Hayslett, T., Bhat, A., and Draper, R.K. (2008). Cholera toxin up-regulates endoplasmic reticulum proteins that correlate with sensitivity to the toxin. Exp. Biol. Med. (Maywood) *233*, 163–175.

Dong, B., Niwa, M., Walter, P., and Silverman, R.H. (2001). Basis for regulated RNA cleavage by functional analysis of RNase L and Ire1p. RNA *7*, 361–373.

Fujinaga, Y., Wolf, A.A., Rodigherio, C., Wheeler, H., Tsai, B., Allen, L., Jobling, M.G., Rapoport, T., Holmes, R.K., and Lencer, W.I. (2003). Gangliosides that associate with lipid rafts mediate transport of cholera and related toxins from the plasma membrane to endoplasmic reticulm. Mol. Biol. Cell *14*, 4783–4793.

Gardner, B.M., and Walter, P. (2011). Unfolded proteins are Ire1-activating ligands that directly induce the unfolded protein response. Science *333*, 1891–1894.

Gonzalez, T.N., Sidrauski, C., Dörfler, S., and Walter, P. (1999). Mechanism of non-spliceosomal mRNA splicing in the unfolded protein response pathway. EMBO J. *18*, 3119–3132.

Hollien, J., and Weissman, J.S. (2006). Decay of endoplasmic reticulum-localized mRNAs during the unfolded protein response. Science *313*, 104–107.

Hollien, J., Lin, J.H., Li, H., Stevens, N., Walter, P., and Weissman, J.S. (2009). Regulated Ire1-dependent decay of messenger RNAs in mammalian cells. J. Cell Biol. *186*, 323–331.

Imagawa, Y., Hosoda, A., Sasaka, S., Tsuru, A., and Kohno, K. (2008). RNase domains determine the functional difference between IRE1alpha and IRE1beta. FEBS Lett. *582*, 656–660.

Iwawaki, T., Hosoda, A., Okuda, T., Kamigori, Y., Nomura-Furuwatari, C., Kimata, Y., Tsuru, A., and Kohno, K. (2001). Translational control by the ER transmembrane kinase/ribonuclease IRE1 under ER stress. Nat. Cell Biol. *3*, 158–164.

Jobling, M.G., and Holmes, R.K. (2001). Biological and biochemical characterization of variant A subunits of cholera toxin constructed by site-directed mutagenesis. J. Bacteriol. *183*, 4024–4032.

Kaser, A., Lee, A.H., Franke, A., Glickman, J.N., Zeissig, S., Tilg, H., Nieuwenhuis, E.E., Higgins, D.E., Schreiber, S., Glimcher, L.H., and Blumberg, R.S. (2008). XBP1 links ER stress to intestinal inflammation and confers genetic risk for human inflammatory bowel disease. Cell *134*, 743–756.

Kato, H., Takeuchi, O., Mikamo-Satoh, E., Hirai, R., Kawai, T., Matsushita, K., Hiiragi, A., Dermody, T.S., Fujita, T., and Akira, S. (2008). Length-dependent recognition of double-stranded ribonucleic acids by retinoic acid-inducible gene-I and melanoma differentiation-associated gene 5. J. Exp. Med. *205*, 1601–1610.

Kawai, T., and Akira, S. (2008). Toll-like receptor and RIG-I-like receptor signaling. Ann. N Y Acad. Sci. *1143*, 1–20.

Lee, A.H., Iwakoshi, N.N., and Glimcher, L.H. (2003). XBP-1 regulates a subset of endoplasmic reticulum resident chaperone genes in the unfolded protein response. Mol. Cell. Biol. *23*, 7448–7459.

Lencer, W.I., Delp, C., Neutra, M.R., and Madara, J.L. (1992). Mechanism of cholera toxin action on a polarized human intestinal epithelial cell line: role of vesicular traffic. J. Cell Biol. *117*, 1197–1209.

Li, T., Diner, B.A., Chen, J., and Cristea, I.M. (2012). Acetylation modulates cellular distribution and DNA sensing ability of interferon-inducible protein IFI16. Proc. Natl. Acad. Sci. USA *109*, 10558–10563.

Lindenbach, B.D., Evans, M.J., Syder, A.J., Wölk, B., Tellinghuisen, T.L., Liu, C.C., Maruyama, T., Hynes, R.O., Burton, D.R., McKeating, J.A., and Rice, C.M. (2005). Complete replication of hepatitis C virus in cell culture. Science *309*, 623–626.

Loo, Y.M., and Gale, M., Jr. (2011). Immune signaling by RIG-I-like receptors. Immunity *34*, 680–692.

Malathi, K., Dong, B., Gale, M., Jr., and Silverman, R.H. (2007). Small self-RNA generated by RNase L amplifies antiviral innate immunity. Nature *448*, 816–819.

Malathi, K., Saito, T., Crochet, N., Barton, D.J., Gale, M., Jr., and Silverman, R.H. (2010). RNase L releases a small RNA from HCV RNA that refolds into a potent PAMP. RNA *16*, 2108–2119.

Martinon, F., Chen, X., Lee, A.H., and Glimcher, L.H. (2010). TLR activation of the transcription factor XBP1 regulates innate immune responses in macrophages. Nat. Immunol. *11*, 411–418.

Pahl, H.L., Sester, M., Burgert, H.G., and Baeuerle, P.A. (1996). Activation of transcription factor NF-kappaB by the adenovirus E3/19K protein requires its ER retention. J. Cell Biol. *132*, 511–522.

Poeck, H., Bscheider, M., Gross, O., Finger, K., Roth, S., Rebsamen, M., Hannesschläger, N., Schlee, M., Rothenfusser, S., Barchet, W., et al. (2010). Recognition of RNA virus by RIG-I results in activation of CARD9 and inflammasome signaling for interleukin 1 beta production. Nat. Immunol. *11*, 63–69.

Rehwinkel, J., and Reis e Sousa, C. (2010). RIGorous detection: exposing virus through RNA sensing. Science *327*, 284–286.

Richardson, C.E., Kooistra, T., and Kim, D.H. (2010). An essential role for XBP-1 in host protection against immune activation in C. elegans. Nature *463*, 1092–1095.

Ron, D., and Walter, P. (2007). Signal integration in the endoplasmic reticulum unfolded protein response. Nat. Rev. Mol. Cell Biol. *8*, 519–529.

Sandvig, K., Garred, Ø., Prydz, K., Kozlov, J.V., Hansen, S.H., and van Deurs, B. (1992). Retrograde transport of endocytosed Shiga toxin to the endoplasmic reticulum. Nature *358*, 510–512.

Saslowsky, D.E., Cho, J.A., Chinnapen, H., Massol, R.H., Chinnapen, D.J., Wagner, J.S., De Luca, H.E., Kam, W., Paw, B.H., and Lencer, W.I. (2010).

Intoxication of zebrafish and mammalian cells by cholera toxin depends on the flotillin/reggie proteins but not Derlin-1 or -2. J. Clin. Invest. *120*, 4399–4409.

Sun, Q., Sun, L., Liu, H.H., Chen, X., Seth, R.B., Forman, J., and Chen, Z.J. (2006). The specific and essential role of MAVS in antiviral innate immune responses. Immunity *24*, 633–642.

Tsai, B., Rodighiero, C., Lencer, W.I., and Rapoport, T.A. (2001). Protein disulfide isomerase acts as a redox-dependent chaperone to unfold cholera toxin. Cell *104*, 937–948.

Urano, F., Wang, X., Bertolotti, A., Zhang, Y., Chung, P., Harding, H.P., and Ron, D. (2000). Coupling of stress in the ER to activation of JNK protein kinases by transmembrane protein kinase IRE1. Science *287*, 664–666.

Wernick, N.L., De Luca, H., Kam, W.R., and Lencer, W.I. (2010). N-terminal extension of the cholera toxin A1-chain causes rapid degradation after retrotranslocation from endoplasmic reticulum to cytosol. J. Biol. Chem. *285*, 6145–6152.